

Observation of spin-wave propagation in permalloy microstrips

Andreas Krohn,* Sebastian Mansfeld, Jan Podbielski, Jesco Topp, Wolfgang Hansen, Detlef Heitmann, and Stefan Mendach
*Institut für Angewandte Physik und Mikrostrukturforschungszentrum,
 Universität Hamburg, Jungiusstrasse 11, D-20355 Hamburg, Germany*
 (Dated: November 29, 2021)

We report on the propagation of spin waves in permalloy microstrips. By means of scanning Kerr microscopy combined with continuous microwave excitation, we detect the time evolution of spin-wave interference patterns in an external magnetic field. Assuming transverse spin-wave quantization we can directly measure the amplitude, phase velocity and damping for the corresponding transversal wave mode numbers m . We find that the spin-wave interference pattern is dominated by $m = 0$ and $m = 2$ with phase velocities $v_{\text{ph},0} = 71$ km/s and $v_{\text{ph},2} = 47$ km/s, respectively.

PACS numbers: 75.75.+a, 76.50.+g, 75.30.Ds, 75.50.Bb

Spin dynamics in patterned ferromagnetic elements have gained growing interest since they exhibit fundamental magnetic phenomena. The understanding of these principles is the key for technical applications in the next decades e.g. data storage, sensors or signal processing. Recently increasing interest has been devoted to localization and propagation of spin waves in permalloy (Py) micro and nano structures, e.g. wires [1, 2], arrays of wires and rings [3, 4], films and lattices [5, 6], or even complex 3D shaped structures [7].

Demidov and coworkers [2] recently observed a complex magnetization pattern in transversally magnetized permalloy microstrips employing time integrating micro-focus Brillouin light scattering. They explained their observations by the interference of spin-wave modes which are propagating along the stripe axis with transverse quantization. In this letter we present time and spatially resolved studies on transversally magnetized Py microstrips. By means of scanning Kerr microscopy combined with microwave excitation (FMR-SKM)[8, 9] we obtain experimental access to the time evolution of the spin-wave interference pattern. Assuming spin-wave quantization transverse to the Py microstrips this data allows us to obtain separated images of the interfering spin-wave modes. We can directly measure their amplitude, phase velocity and damping. Our measurements agree well with a dipole-based model for our stripe geometry [10].

Our samples consist of a GaAs substrate with a 200-nm-thick coplanar waveguide (CPW) fabricated on top. As shown in Fig. 1(a) the inner conductor is $3 \mu\text{m}$ wide. The gaps between inner conductor and ground lines are $2.5 \mu\text{m}$ wide. The CPW is planarized and electrically insulated by a 250 nm thick layer of hydrogen silsesquioxane (HSQ). With electron beam lithography and thermal evaporation we place 20-nm-thick, $80 \mu\text{m}$ long and $5 \mu\text{m}$ wide $\text{Ni}_{80}\text{Fe}_{20}$ stripes on top of this dielectric layer, cross-

ing the CPW at right angle.

We utilize the magneto-optic Kerr effect to detect the magnetization dynamics. For this purpose we set up a time-resolved scanning Kerr microscope with a spatial resolution better than $1 \mu\text{m}$ and a temporal resolution better than 1 ps. We use a customized microwave synthesizer (Parzich, ITS-9200) that can be locked to a laser-pulse train with a repetition frequency between 74.1 and 77.9 MHz. This circumvents the need of a stabilizing system for our pulsed laser system (Coherent, Mira900f). The synthesizer generates microwaves be-

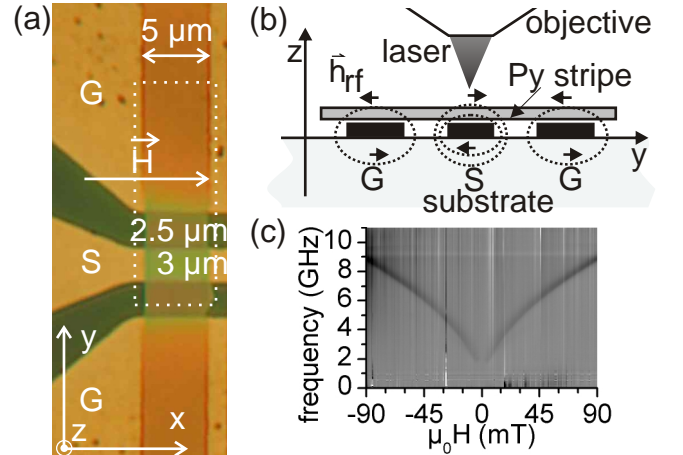


FIG. 1: (color online) (a) Top view micrograph of the 20 nm thick permalloy stripe prepared on top of the coplanar waveguide (CPW). The Py stripe is oriented perpendicular to the signal line (S) and the two ground lines (G) of the CPW. The external field H is applied in x direction perpendicular to the stripe axis. (b) Spin-wave dispersion of the stripe obtained by microwave absorption spectroscopy in Damon-Eschbach geometry (dark lines correspond to strong absorption). (c) Schematic cross-section along the axis of the Py stripe perpendicular to the CPW plane. The high-frequency current driven by the microwave produces a rf-magnetic field that excites spin precession in the Py stripes. The spin precession is stroboscopically detected with focused fs laser pulses via the polar magneto optical Kerr effect with a temporal resolution below 1 ps and a spatial resolution below $1 \mu\text{m}$.

*corresponding author email: andreas.krohn@physnet.uni-hamburg.de

tween 4 and 10 GHz with an increment corresponding to the laser repetition rate of about 76 MHz. The phase between microwave and laser pulses can be adjusted within 2π . In the following experiments we saturate the sample at $\mu_0 H = 90$ mT perpendicular to the stripe axis (Fig. 1(a)) and then decrease the external field to the specified value. First, we determine the spin-wave eigenmode spectrum of the Py stripes by means of broadband microwave spectroscopy (Fig. 1(c)). For a given resonance condition we then pass the laser-locked microwave through the CPW to excite magnetization dynamics in the Py stripes and stroboscopically measure the polar Kerr signal (Fig. 1(b)) [8]. Spatial resolution is obtained by scanning the sample under the focused laser pulses.

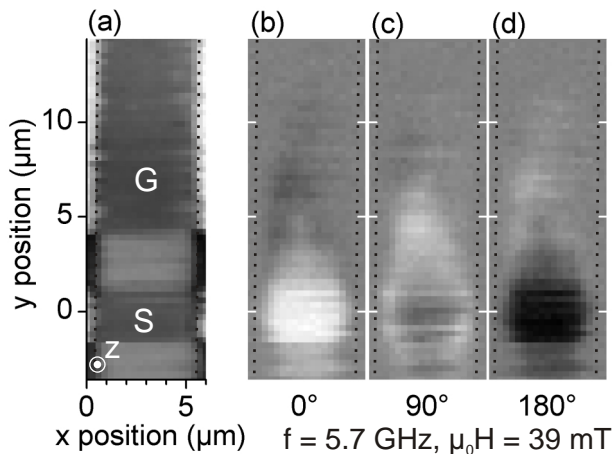


FIG. 2: (a) Scanning reflection image of the sample area marked by the dotted box in Fig. 1(a). Due to different reflectivity of permalloy on gold (dark gray) and permalloy on gallium arsenide (light gray) we can image the CPW below the Py stripe. Pure GaAs and Gold are coded black and white, respectively. (b)-(c) Magnetic-contrast image of the stripe for three different phases between the laser pulses and the microwave excitation. The edges of the stripe are marked by a dotted line. Black and white correspond to the maximum deflection of the spins in opposite directions. The reflection and magnetic-contrast images are mapped simultaneously enabling a precise spatial assignment of the spin-wave pattern.

In Fig. 2 we show data obtained at an excitation frequency of 5.7 GHz at an external field of 39 mT. Figure 2(a) shows a reflection image of the sample that was taken simultaneously to the magnetic-contrast images of the stripe depicted in Fig. 2(b)-(d). In Fig. 2(a) one can clearly identify the signal and ground lines of the CPW as well as the edges of the permalloy stripes (marked with dotted lines). In the magnetic-contrast images we see the polar Kerr rotation corresponding to the z component of the magnetization m_z of the permalloy. Black and white indicate the maximum value on opposite z directions. The three plots in Fig. 2(b)-(d) show three phases of the microwave excitation relative to the probe-laser pulses. In Fig. 2(b) we find a white area at the position of the signal line of the CPW. When the phase ϕ

between laser pulse and microwave is changed by 90 degree (Fig. 2(c)), the white area travels some micrometer along the stripe and changes its transversal profile. At the position of the excitation we do not find a gray area, as expected for a sinusoidal wave, but a pattern of black and white areas. In Fig. 2(d) the phase is shifted another 90 degrees and we observe a black area at the position of the excitation. The white area has moved further on and lost intensity due to damping in the material. In all three magnetic-contrast images we find a vanishing amplitude of the magnetization precession at the edge of the stripes which suggests a strong pinning of the magnetization at these sites.

The transversal profile of the spin wave traveling along the stripe reflects the confinement of the spin wave in the transversal geometry. Following Ref. [2, 11] we assume quantization rules in the form $k_{x,m} = (m+1)\pi/w_{\text{eff}}$ where m is the quantization number and w_{eff} represents the effective width of the stripe. Taking into account that we do not excite modes with odd quantum numbers [12] and that only the two strongest modes $m = 0$ and $m = 2$ are relevant we get the general form of the magnetization:

$$m_z(x, y, t) \propto A_0 \exp(\kappa_0 y) \cos(k_{y,0} y - \omega \Delta t + \varphi_0) \sin\left(\frac{\pi x}{w_{\text{eff}}}\right) + A_2 \exp(\kappa_2 y) \cos(k_{y,2} y - \omega \Delta t + \varphi_2) \sin\left(\frac{3\pi x}{w_{\text{eff}}}\right). \quad (1)$$

Here $k_{y,0}$ and $k_{y,2}$ represent the wave vectors along the stripe axis for the modes $m = 0$ and $m = 2$, A_0 and A_2 are the amplitudes of the modes. φ_0 and φ_2 take into account the phases between the two modes and the microwave excitation. κ_0 and κ_2 are specific damping parameters. $\omega = 2\pi f$ is related to the excitation frequency of the microwave. Since our magnetic-contrast images are taken along the x axis in subsequent line scans, we fit our data for fixed y values. Figure 3(a) shows the magnetization m_z in arbitrary units for several time steps (dots) together with the fitted curves from Eq. (1) (lines) for $y = 0$. As we know the frequency of the microwave we can transform the phase shift $\Delta\phi$ between microwave and laser pulses into a time interval $\Delta t = \Delta\phi/\omega$. With the fitting parameters A_0 , A_2 , $(k_{y,0} \cdot y)$, $(k_{y,2} \cdot y)$, φ_0 and φ_2 for all y positions we can separate the two dominant modes. Comparing the amplitudes we find the higher mode to be four times weaker than the fundamental mode which reflects the decrease in oscillator strength of the confined spin wave with increasing mode number [12]. The phase shift between the modes is $|\varphi_0 - \varphi_2| = 128^\circ$. Using these parameters, we can construct 2D plots of the individual modes for every time step. Figure 3(b) and (d) show the separated modes at $\Delta t = 44$ ps. In the area covering the signal line (white, dashed rectangle) the magnetization is driven by the microwave. We extract the damping parameters from the decrease of the transversally integrated spin-wave intensity along the stripe, starting at the edge of the signal line. With $\kappa_0 = \kappa_2 = -0.25 \mu\text{m}^{-1}$

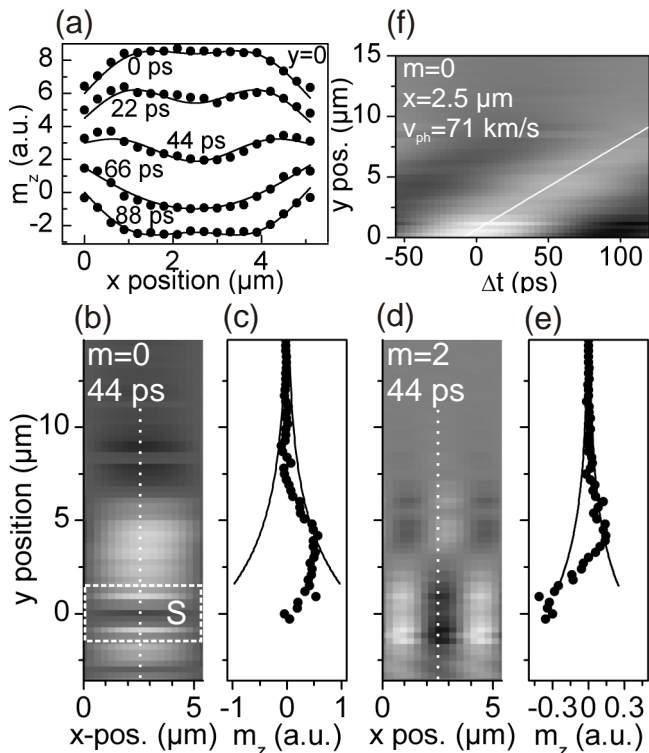


FIG. 3: (a) z component of the magnetization across the Py stripe at $y = 0$ along the x direction for five different phase steps, i.e., points in time. Circles correspond to the Kerr signal, lines correspond to fits with Eq. (1). (b),(d) Patterns of the separated modes obtained from the fitting parameters (A_0 , A_2 , $(k_{y,0} \cdot y)$, $(k_{y,2} \cdot y)$, φ_0 and φ_2) at 44 ps. The signal line is marked with the white rectangle. (c),(e) cross-section along the stripe (dotted lines in (b),(d)) and damping curves. (f) Temporal evolution of the cross-section along the stripe. The slope of the white area (white line) represents the phase velocity of the mode and corresponds to a wave vector $k = 0.5 \cdot 10^4 \text{ cm}^{-1}$.

we receive identical values for the damping of both modes within the accuracy of the measurement. Figure 3(c) and (d) show a cross-section along the center of the stripe (dotted line in Fig. 3(b) and (d)) together with the corresponding damping curves. From the time evolution of these plots we can directly measure the phase velocity of the individual modes. To extract the phase velocity we plot a cross-section along the center of the stripe (dotted line in Fig. 3(b)) over time Δt (Fig. 3(f)). From the slope of the white area we obtain the phase velocity of the respective mode. For the mode $m = 0$ we determine a phase velocity of $v_{\text{ph},0} = 71 \text{ km/s}$ and for the mode $m = 2$ we find $v_{\text{ph},2} = 47 \text{ km/s}$ corresponding to wave vectors $k_0 = 0.5 \cdot 10^4 \text{ cm}^{-1}$ and $k_2 = 0.77 \cdot 10^4 \text{ cm}^{-1}$, respectively. This is in good agreement with calculations on the dispersion relations of spin-wave modes based on the dipole-exchange model [11] for our stripe geometry.

In conclusion, we have shown time and spatially resolved measurements of spin waves in transversally magnetized permalloy stripes obtained with a combination of scanning Kerr microscopy and continuous microwave excitation. Spin-wave confinement in the stripes leads to spin-wave modes with different wave vectors that travel along the stripe producing a characteristic interference pattern. These experiments allow us to separate the individual spin-wave modes in the time and spatial domain and to extract amplitude, phase velocity, and damping of the respective modes. The obtained data is in good agreement with a dipole-exchange based model for the spin-wave dispersion in Py microstrips.

This work was supported by the DFG via SFB 668, SFB 508 and GrK 1286.

-
- [1] V. E. Demidov, S. O. Demokritov, K. Rott, P. Krzyteczko, and G. Reiss, *Applied Physics Letters* **92**, 232503 (2008).
 - [2] V. E. Demidov, S. O. Demokritov, K. Rott, P. Krzyteczko, and G. Reiss, *Physical Review B* **77**, 064406 (2008).
 - [3] J. Topp, J. Podbielski, D. Heitmann, and D. Grundler, *Physical Review B* **78**, 024431 (2008).
 - [4] F. Giesen, J. Podbielski, T. Korn, and D. Grundler, *Journal Of Applied Physics* **97**, 10A712 (2005).
 - [5] K. Perzlmaier, G. Woltersdorf, and C. H. Back, *Physical Review B* **77**, 054425 (2008).
 - [6] S. Neusser, B. Botters, M. Becherer, D. Schmitt-Landsiedel, and D. Grundler, *Applied Physics Letters* **93**, 122501 (2008).
 - [7] S. Mendach, J. Podbielski, J. Topp, W. Hansen, and D. Heitmann, *Applied Physics Letters* **93**, 262501 (2008).
 - [8] S. Tamaru, J. A. Bain, R. J. M. van de Veerdonk, T. M. Crawford, M. Covington, and M. H. Kryder, *Journal Of Applied Physics* **91**, 8034 (2002).
 - [9] I. Neudecker, M. Klau, K. Perzlmaier, D. Backes, L. J. Heyderman, C. A. F. Vaz, J. A. C. Bland, U. Rudiger, and C. H. Back, *Physical Review Letters* **96**, 057207 (2006).
 - [10] K. Y. Guslienko, S. O. Demokritov, B. Hillebrands, and A. N. Slavin, *Physical Review B* **66**, 132402 (2002).
 - [11] K. Y. Guslienko, R. W. Chantrell, and A. N. Slavin, *Physical Review B* **68**, 024422 (2003).
 - [12] C. Kittel, *Physical Review* **110**, 1295 (1958).